Geophysical Research Letters

RESEARCH LETTER
10.1029/2020GL089274

Drivers of Subsurface Deoxygenation in the Southern California Current System

Natalya Evans[1], Isaac D. Schroeder[2,3], Mercedes Pozo Buil[2,3], Michael G. Jacox[3,4], and Steven J. Bograd[3]

[1]Department of Biological Sciences, University of Southern California, Los Angeles, CA, USA, [2]Institute of Marine Sciences, University of California, Santa Cruz, CA, USA, [3]Environmental Research Division, NOAA Southwest Fisheries Science Center, La Jolla, CA, USA, [4]Physical Sciences Laboratory, NOAA Earth System Research Laboratories, Boulder, CO, USA

Abstract A confluence of subarctic, tropical, and subtropical water masses feed the California Current System (CCS), supporting a highly productive ecosystem and wide array of marine ecosystem services. Long-term declines in oxygen have been observed in this region, causing habitat compression and other ecosystem consequences. Here we quantify the water masses and processes causing deoxygenation in the subsurface CCS from 1993–2018, and we find that deoxygenation was caused both by changes in the advection of source waters and increased remineralization in the source waters. The historical deoxygenation trend can be attributed primarily (81%) to the Northern Equatorial Pacific Intermediate Water, the deep Pacific Equatorial Water mass transported in the California Undercurrent. We also find that advection and remineralization share nearly equal contributions to deoxygenation. This improved understanding of the mechanisms affecting the aerobic habitat of the CCS will inform projections of ecological impacts and mitigation of future deoxygenation.

Plain Language Summary The California Current System (CCS) supports rich populations of finfish and marine invertebrates, rendering it ecologically and economically important. Climate change threatens these populations with increased temperatures, more acidic waters, and lower oxygen concentrations. From 1993 to 2018, we found the mean oxygen concentration in the southern, subsurface CCS decreased by 25%. This decrease can be attributed to the contributions of six water masses that feed the CCS, though they originate far afield in the Pacific Ocean. We discovered that from 1993–2018, 24 μM of deoxygenation occurred, and 81% of the observed deoxygenation was caused by a single water mass, the Northern Equatorial Pacific Intermediate Water. This water mass is transported into the CCS from the Eastern Tropical North Pacific via the California Undercurrent. Within the 81% of observed deoxygenation, 24% was caused by internal changes within the core of this water mass before it reached the CCS, likely in the Eastern Tropical North Pacific off Mexico. Understanding the drivers that influence oxygen availability in the CCS will assist with efforts to simulate biogeochemical changes. It will also improve projections about the ways that deoxygenation will impact this ecosystem and inform possibilities to mitigate future deoxygenation caused by climate change.

Key Points:
- Source water masses are responsible for -0.92 ± 0.04 μM year^{-1} of deoxygenation in the subsurface, southern CCS
- Northern Equatorial Pacific Intermediate Water drove 81% (-0.78 ± 0.05 μM year^{-1}) of deoxygenation in the southern CCS from 1993 to 2018
- Outside of the CCS, remineralization within source water masses caused 32% (-0.31 ± 0.04 μM year^{-1}) of deoxygenation

Supporting Information:
- Supporting Information S1

Correspondence to:
N. Evans,
n.evans@usc.edu

Citation:
Evans, N., Schroeder, I. D., Pozo Buil, M., Jacox, M. G., & Bograd, S. J. (2020). Drivers of subsurface deoxygenation in the southern California Current System. *Geophysical Research Letters*, *46*, e2020GL089274. https://doi.org/10.1029/2020GL089274

Received 19 JUN 2020
Accepted 1 OCT 2020
Accepted article online 9 OCT 2020

Author Contributions:
Data curation: Isaac D. Schroeder, Mercedes Pozo Buil, Michael G. Jacox, Steven J. Bograd
Formal analysis: Natalya Evans
Writing - original draft: Natalya Evans, Steven J. Bograd
Writing – review & editing: Isaac D. Schroeder, Mercedes Pozo Buil, Michael G. Jacox, Steven J. Bograd

1. Introduction

The California Current System (CCS), a coastal upwelling biome off the west coast of the United States, supports a highly productive ecosystem and a wide array of marine ecosystem services. These ecosystem services include storm protection, pollution control, food, recreation, and carbon sequestration (Barbier, 2017). Climate change is expected to impact the CCS by raising temperatures, lowering oxygen concentrations, and causing more acidic waters, all of which change ecosystem productivity, structure, and function (Deutsch et al., 2015; Howard et al., 2020; Koslow et al., 2013). Off Southern California, long oceanographic time series have documented significant physical and biogeochemical variability; trends in subsurface warming and deoxygenation have corresponded with enriched nutrients and enhanced acidification (Bograd et al., 2008, 2015; McClatchie et al., 2010; Meinvielle & Johnson, 2013; Nam et al., 2015; others). This biogeochemical variability is consistent with the effects expected from climate change: warmer waters reducing oxygen solubility, increasing water column stratification limiting ocean ventilation, and accelerating oxygen consumption via respiration (Breitburg et al., 2018; Brewer & Peltzer, 2016; Doney et al., 2012;

Gruber, 2011; Keeling et al., 2010; Levin, 2018). While several studies have suggested that the observed biogeochemical trends are associated with changes in the properties and/or advection of source waters to the CCS (Bograd et al., 2015, 2019), the explicit processes and water masses causing deoxygenation have not been quantified.

A recent study performed an extended optimum multiparameter analysis (eOMP) (Tomczak & Large, 1989) on the long-term hydrographic data from the California Cooperative Oceanic Fisheries Investigations (CalCOFI) program to quantify the spatiotemporal variability of source water contributions to the southern CCS (Bograd et al., 2019). That study described the distribution of six source water masses that feed the southern CCS and found significant long-term variability in the relative contribution and distribution of upper and deeper Pacific Equatorial Waters (PEW). These water masses are transported to the CCS within the California Undercurrent (CUC), and they are relatively low in oxygen relative to the other water masses (Bograd et al., 2019, Meinvielle & Johnson, 2013). In this study, we extended this eOMP by framing deoxygenation as a function of water mass contributions, which allowed us to quantify the relative contributions of different processes, specifically changes in the advection of source water masses versus remineralization accompanying these source water masses. Improving our understanding of deoxygenation in the CCS will highlight priorities for simulation developments that can better project biogeochemistry in the region, informing potential mitigation strategies.

2. Methods

2.1. Data From the Southern CCS

We used historical hydrographic data from the CalCOFI program, which has consistently sampled the southern CCS from San Diego to Pt. Conception quarterly since 1984, with target months of January, April, July, and October (Figure 1), amounting to more than 6,700 station occupations from 1984–2018. Parameters measured include temperature (T), salinity (S), oxygen (O_2), nitrate (NO_3), phosphate (PO_4), and silicate (SiO_4). CalCOFI sampling extends to 500 m or the continental shelf, if shallower. Further details can be found in any of the CalCOFI data reports or online (at www.calcofi.org).

2.2. Optimum Multiparameter Analysis in the CCS

OMP analysis (Tomczak & Large, 1989) estimates the relative contributions of source water types that mix together to form an observed water mass, assuming that water mass properties are quasi-conservative. In extended OMP (eOMP) analysis, nutrient concentrations for each water mass are set at a location upstream of the location of interest (Anderson & Sarmiento, 1994; Brzezinski, 1985; Karstensen & Tomczak, 1997), and the change in phosphate, ΔP, accounts for nutrient concentration changes along the advective pathway (García-Ibáñez et al., 2015; Poole & Tomczak, 1999). ΔP is related to changes in oxygen, nitrate, and silicate through Redfield ratios (Anderson & Sarmiento, 1994; Brzezinski, 1985) that occur due to organic matter remineralization. Bograd et al. (2019) performed eOMP on the 1984–2018 CalCOFI data. They first defined six source water masses using three 10° × 10° boxes centered at 45°N, 135°W with depths of 101 and 178 m; 27°N, 139°W with depths of 85 and 219 m; and 5°N, 108°W with depths of 131 and 399 m, corresponding to Pacific Subarctic Upper Waters (PSUW), Eastern North Pacific Central Waters (ENPCW), and PEW, respectively. Each of these three locations has an upper and a deeper water mass, denoted uPSUW and dPSUW, respectively. They obtained available data within each source water box from the World Ocean Database 2018. While these three boxes act as the source regions for water masses entering the CCS, these boxes are not the ultimate formation regions for these six water masses.

With six source water masses, defined as time-invariant using WOD18 data from 1984–2018, and six input parameters (T, *S*, O_2, NO_3, PO_4, and SiO_4), Bograd et al. (2019) solved for the relative contributions of each water mass at each CalCOFI station, depth, and sampling time. During these calculations, ΔP is estimated using the equations in Bograd et al. (2019) for each sample, such that each station and depth has its own ΔP value. This ΔP term allows us to calculate the extent that remineralization has accumulated in source water masses to the CalCOFI region after water mass formation. To deconvolute the drivers of this deoxygenation signal, we averaged water mass contribution for each sample from 100 to 400 m depth across every station for a given season and a given year. Beyond these depths, the eOMP error was greater than 10%, and

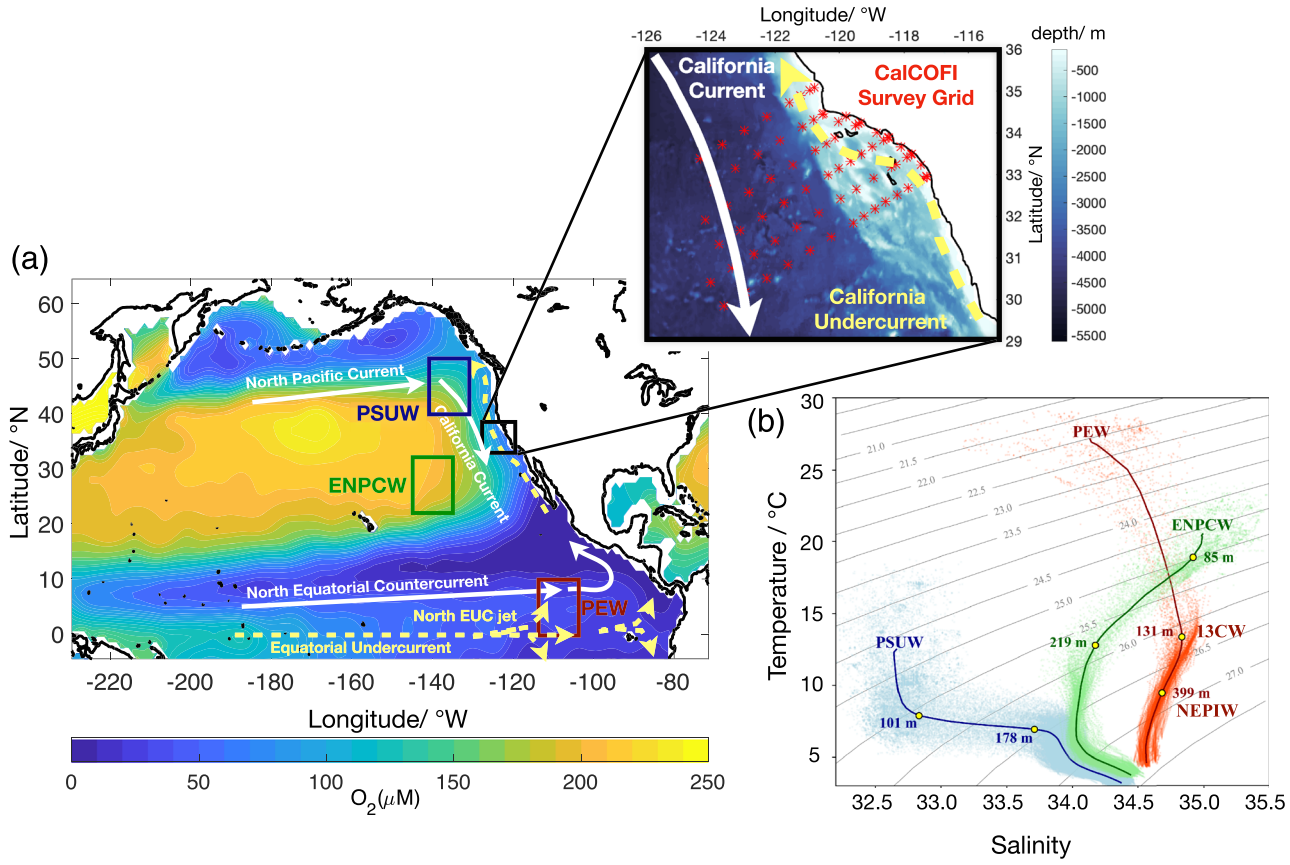

Figure 1. (a) Map of the annual climatology of O_2 at 300 m in the North Pacific for the period 1955–2017, with the regions where we defined upper and deeper PSUW (blue box), ENPCW (green box), and PEW (red box). The map illustrates the main surface (white) and subsurface (yellow dotted) currents. O_2 data obtained from WOA18 (Garcia et al., 2013). The inset map highlights the nominal CalCOFI survey grid and bathymetry of the region, obtained from ETOPO2 (National Geophysical Data Center, 2006). (b) TS diagram for PSUW (blue), ENPCW (green), and PEW or 13CW/NEPIW (red), modified from Bograd et al. (2019).

therefore these samples were omitted from this analysis. Since there is significant seasonal variability in the subsurface CCS (Nam et al., 2015), we analyzed each season individually for long-term trends.

Here we note that the upper and deeper PEW source waters used in Bograd et al. (2019, supporting information Table S1) are more broadly referred to as 13°C Water (13CW) and Northern Equatorial Pacific Intermediate Water (NEPIW), following Evans et al. (2020). We will use this nomenclature as it better represents these water masses within the Pacific Ocean and links them to other papers that describe their sources and transport (Bostock et al., 2010; Fiedler & Talley, 2006; Qu et al., 2009; Tsuchiya, 1981; others). Evans et al. (2020) contains additional references discussing these water masses.

2.3. Linking Water Masses to Deoxygenation

eOMP deconvolutes observed hydrographic properties into a ratio of source water masses and an amount of remineralization. The ratio of source water masses sets the maximum possible O_2 while remineralization lowers it to the observed value. In this paper, advective (de)oxygenation refers to changes in O_2 caused only by changing the ratio of source water contributions. While eOMP does not attribute remineralization to specific water masses, this was a primary goal for this analysis. For this purpose, we separated the OMP-derived remineralization into two categories: internal and advection-derived. Internal remineralization refers to ΔP that has accumulated within each water mass, independent of each other, between their formation regions and the CCS. Advection-derived remineralization refers to a change in the amount of ΔP accumulated within the CCS because the ratio of water mass contributions has changed. Our results indicate that the source water masses experience different amounts of ΔP between their defined source regions and the CCS, and as advection alters the ratio of water mass contributions, it also alters the ΔP observed in the

CCS as a function of these contributions. Equation 1 depicts the deconvolution we performed to identify the causes of deoxygenation in the southern CCS, where the first term refers to advective (de)oxygenation, whereas the second and third terms are internal and advection-derived remineralization, appropriately. Bold variables represent matrices, whereas plain text variables represent scalars or vectors.

$$\frac{d[O_2]}{dt} = \left(\frac{\partial \boldsymbol{x}}{\partial t}\right)\boldsymbol{O_{2,x}} + \left(\frac{-170\ \mu M\ O_2}{\mu M\ \boldsymbol{\Delta} P}\right)\left(\left(\frac{\partial(\boldsymbol{\Delta} P)}{\partial t}\right)_{\boldsymbol{x}} + \left(\frac{\partial(\boldsymbol{\Delta} P)}{\partial \boldsymbol{x}}\right)_{t}\left(\frac{\partial \boldsymbol{x}}{\partial t}\right)\right). \quad (1)$$

To determine advective (de)oxygenation, we calculated the theoretical O_2 concentration that would be present in the CCS given the contributions of each water mass without remineralization. We compared this to the O_2 concentration if one of the water masses did not contribute. While completely omitting one of these water masses is unrealistic for the CCS, these calculations are intended to generate a long-term trend for how changes in source water mass advection change the concentration of O_2 rather than an absolute value.

Remineralization lowers the O_2 concentration during the transport of each water mass as well as locally in the CCS. Within a water mass, increased remineralization due to elevated temperatures is the most prevalent cause of deoxygenation (Brewer & Peltzer, 2016), but changes in production, export, and surface warming can also alter properties within a water mass (Rykaczewski & Dunne, 2010). Mathematically, eOMP groups these processes into the ΔP term, and stoichiometrically scaling this parameter by $-170\frac{\mu M\ O_2}{\mu M\ PO_4}$ provides the deoxygenation from remineralization, as this scaling factor was implemented in the eOMP in Bograd et al. (2019). For each season and year, we averaged a given property, such as O_2 (Figure 1) or a water mass contribution, across all stations and depths from 100–400 m, and we presented these values as time series for each season.

The deoxygenation from accumulated internal remineralization within each water mass is quantified by tracking how much remineralization varies over time in the core of each water mass. Since we deconvoluted these water masses from CCS data and the maximum contribution of each water mass differs significantly, we analyzed the amount of O_2 lost from remineralization at the same quantile for each water mass. Quantiles are useful because the contributions of NEPIW and dPSUW changed monotonically across this time period, so we must implement a threshold below the absolute maxima of each water mass. We analyzed remineralization between the 84% and 85% quantiles to ensure all years of the analysis were represented, and justifications for this quantile selection are discussed in detail within the SI. For these calculations, samples with water mass contributions corresponding to 84–85% of each water mass were selected, and the ΔP calculated for these samples was averaged and scaled stoichiometrically to O_2.

Deoxygenation from advection-derived remineralization was calculated by deconvoluting the OMP-derived ΔP term into components for each water mass. Each water mass component was then regressed linearly over time to determine how changes in the advection of that water mass into the CCS influenced the accumulated remineralization. Years with greater than 20% error from the initial OMP-derived remineralization were omitted, as presented in Figure S5c. These data were deconvoluted using singular value decomposition (SVD), as described in Glover et al. (2011), with the source water mass contributions. All linear regressions performed in this paper were Type 1 using code provided in Glover et al. (2011), and linear regressions were performed on combined data from all seasons.

3. Results

3.1. Impact of Advection Versus Remineralization on Deoxygenation

In the southern, subsurface CCS between 100 and 400 m, we found that $0.97 \pm 0.09\ \mu M\ year^{-1}$ of deoxygenation occurred from 1993–2018, and this value matches with depth-dependent estimates in Bograd et al. (2008).

NEPIW is the only water mass driving advective (de)oxygenation, as it has the lowest O_2 concentration of the six water masses and the contribution of this water mass monotonically increases. Increasing NEPIW advection caused $-0.487 \pm 0.001\ \mu M\ year^{-1}$ of deoxygenation (Figure 2b). The total deoxygenation in the CCS can be reconstructed by summing the $-0.44 \pm 0.04\ \mu M\ year^{-1}$ of deoxygenation from accumulated

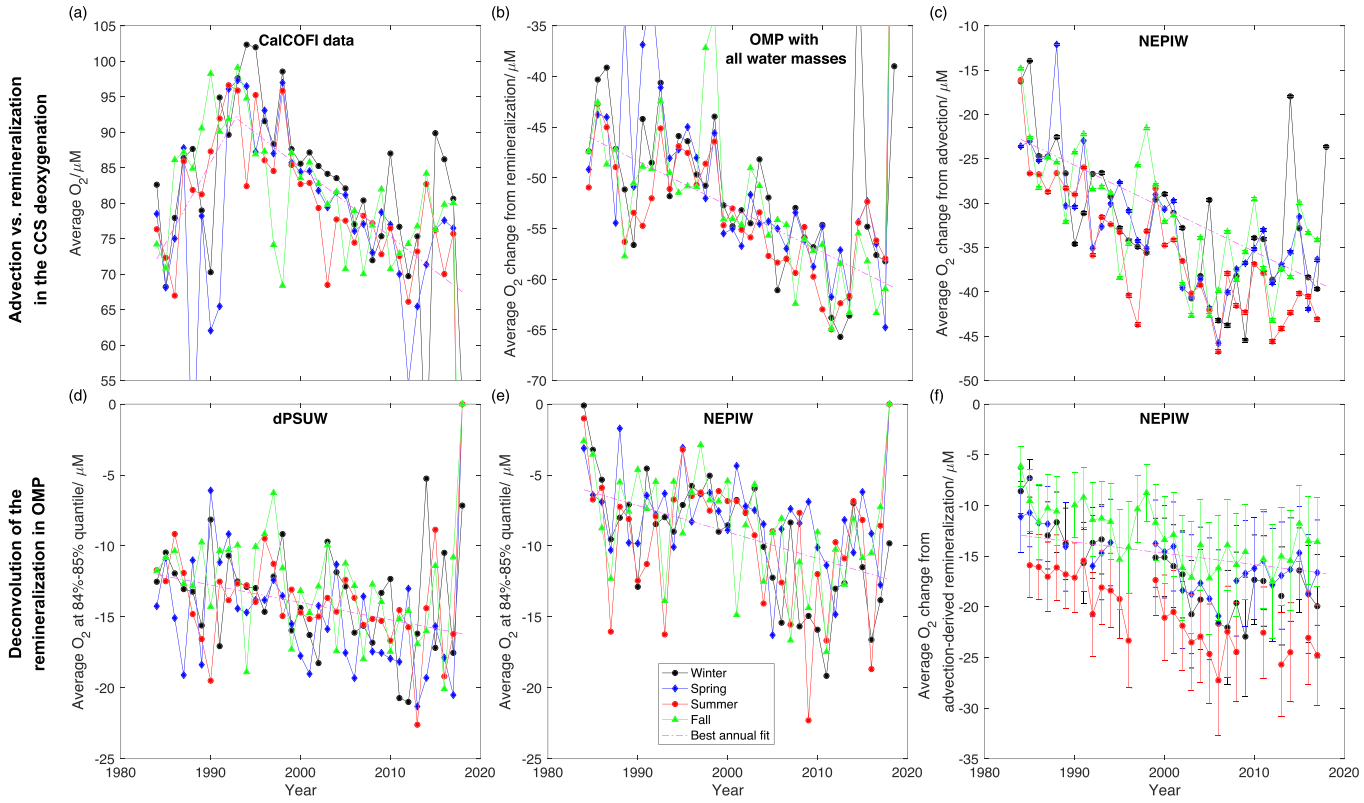

Figure 2. (a) Mean O_2 measured in the CalCOFI study region between 100 and 400 m. Oxygenation occurs from 1985–1993 at 2.3 ± 0.6 μM year^{-1} and deoxygenation occurs from 1993–2018 at −0.97 ± 0.09 μM year^{-1}. The deoxygenation trend in (a) is reconstructed by both (b) mean advective (de)oxygenation from NEPIW with a long-term trend of −0.487 ± 0.001 μM year^{-1} and (c) deoxygenation from remineralization calculated in eOMP with a long-term trend of −0.44 ± 0.04 μM year^{-1}. Since eOMP does not attribute remineralization to specific water masses, (c) is further deconvoluted in (d)–(f). (d) O_2 lost through accumulated internal remineralization in dPSUW with a long-term trend of −0.12 ± 0.03 μM year^{-1} and (e) O_2 lost through internal remineralization in NEPIW with a long-term trend of −0.20 ± 0.03 μM year^{-1}. (f) Deoxygenation caused by water mass advection-derived remineralization from NEPIW with a long-term trend of −0.11 ± 0.04 μM year^{-1}. Uncertainties were not determined for (b) and values less than 40 μM were not included in the fit. Error bars for (c) consist of the uncertainty in the water mass contribution combined with the uncertainty in the NEPIW O_2 water mass definition, but these error bars are too small to be seen. Error bars are not presented for (a), (d), and (e). Error bars in (f) present the uncertainty in the SVD fit propagated through the water mass contribution.

remineralization calculated in the eOMP (Figure 2c) and the advective (de)oxygenation from NEPIW (Figure 2a). This reconstructed total deoxygenation is −0.92 ± 0.04 μM year^{-1}, which is statistically similar to the −0.97 ± 0.09 μM year^{-1} observed from 1993–2018 in the O_2 data, presented in Figure 2a. This treatment matches the observed deoxygenation and increased advection of NEPIW is responsible for 50% of the deoxygenation from 1993–2018, such that it shares nearly equal contribution with accumulated remineralization.

Oxygenation from 1984–1993 can be attributed to the advection of both PSUW water masses, which have the highest O_2 concentrations of the six water masses. This oxygenation trend is most clear in uPSUW from 1984–1993, though dPSUW reached a relative minimum in deoxygenation in the late 1980s. Fitting these individual time periods yields oxygenation trends of 0.62 ± 0.07 μM year^{-1} for uPSUW and 1.1 ± 0.5 μM year^{-1} for dPSUW, causing a net oxygenation of 1.7 ± 0.6 μM year^{-1}, compared to the 2.3 ± 0.6 μM year^{-1} calculated from the CalCOFI data set in Figure 2a. The magnitude of dPSUW suggests that it is primarily responsible for this oxygenation trend; however, it leads to deoxygenation after 1989, unlike the 1984–1993 trend observed in the CalCOFI data. While the magnitude of oxygenation can be explained via these two water masses, the scatter in dPSUW deoxygenation undercuts this conclusion, such that we cannot fully explain the early oxygenation trend with these results. Figure S2 and Table S2 expand on this information. This trend of CCS oxygenation sharply switching to deoxygenation at 1993 is remarkably similar to that of $\Delta\delta^{15}N$ measurements of particulate organic nitrogen in sediments from Baja California and

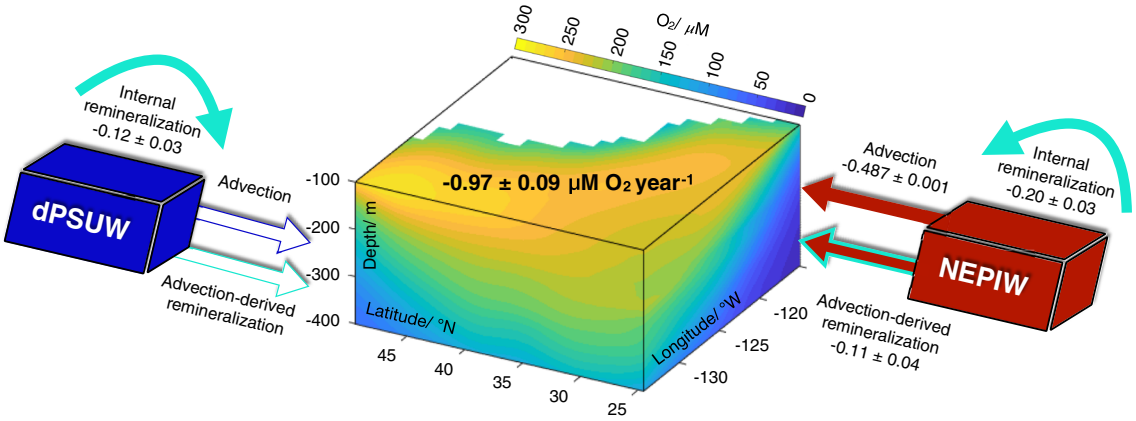

Figure 3. Summary schematic for the processes and contributions of dPSUW and NEPIW on deoxygenation in the CCS, with the amount of deoxygenation written next to each relevant process. On the left, all three processes are linked to dPSUW but it only impacts deoxygenation through accumulated internal remineralization, hence the solid arrow. On the right, NEPIW actively contributes to deoxygenation through all three processes. Advection-derived remineralization is highlighted in light blue because the OMP deconvolutes it as remineralization, but it depends on increased NEPIW advection from 1984–2018.

the Santa Monica Basin (Deutsch et al., 2014). These measurements were used as a proxy for the size of the Eastern Tropical North Pacific Oxygen Deficient Zone (ETNP ODZ), and Deutsch et al. attributed these $\Delta\delta^{15}$N-PON trends to equatorial wind stress weakening, then intensifying. Based on the similarity of this data to O_2 concentrations in the CCS and the connection of these regions, this equatorial wind stress likely influences the CCS as well and is worth further investigation.

3.2. Deconvoluting Accumulated Remineralization Within Water Masses

The eOMP results suggest that remineralization has accumulated most in the deepest waters, particularly below 300 m (Figure S2a). This depth range corresponds to dPSUW and NEPIW (Figures S2b and S2c), so internal remineralization within the dPSUW and NEPIW are most significant to accumulated remineralization in the southern CCS. Internal remineralization within other water masses has less influence on the average O_2 concentration of the region but could be important in specific locations. At the 84–85% quantile, the dPSUW water mass contributes 81%, while the NEPIW water mass only contributes 37%, as seen in Figure S3.

The accumulation of internal remineralization in the dPSUW has increased monotonically during the study time (Figure 2d). This process appears more seasonally variable in the NEPIW (Figure 2e) than the dPSUW, and other nonmonotonic factors appear to influence it in NEPIW, as seen by the lower scatter from 1994–2004. The increased accumulation of internal remineralization in the NEPIW is approximately 1.5x that of the dPSUW, which could be a function of the organic carbon flux into these water masses or the temperature difference between the two water masses. The NEPIW is transported into the southern CCS from the shadow zone around the ETNP ODZ. This internal remineralization likely occurs in that region off Mexico, since the circulation is sluggish and the residence time of this water mass is long.

3.3. Deoxygenation From Water Mass Advection-Derived Remineralization

Each of the source water masses entering the southern CCS accumulates a different amount of remineralization as it is advected from the source location to the CCS. Therefore, changing the ratio of water mass contributions to the CCS also changes the accumulated remineralization calculated in eOMP. NEPIW was found to be the only significant contributor to advection-derived remineralization with -0.11 ± 0.04 μM year^{-1} (Figure 2f). The advection-derived remineralization and the accumulated internal remineralization calculated in section 3.2 sum to -0.42 ± 0.05 μM year^{-1} while the eOMP calculated -0.44 ± 0.04 μM year^{-1} of deoxygenation, suggesting that these deconvolutions reproduce the deoxygenation from eOMP remineralization with statistical significance.

4. Discussion

Climate change-driven deoxygenation is a significant stressor on the global ocean, with eastern boundary upwelling systems being particularly vulnerable regions. The consequences of deoxygenation have already

been observed within the CCS (Koslow et al., 2011, 2013). We analyzed the drivers of deoxygenation in the CCS through water mass deconvolution of the CalCOFI data set (Bograd et al., 2019). We found that the average O_2 concentration in the subsurface CCS increased by 20 ± 5 μM from 1985–1993 and decreased by 24 ± 2 μM from 1993–2018. By quantifying deoxygenation as a function of water masses, we observed that advection and remineralization share nearly equal impact in causing deoxygenation in the CCS.

Figure 3 illustrates the processes and water masses that have caused deoxygenation in the CCS from 1993–2018. NEPIW is responsible for 81% (-0.78 ± 0.05 μM year^{-1}) of deoxygenation from 1984–2018 with elevated summer impacts. The average contribution of NEPIW to the CCS has increased monotonically since 1984 and this increased advection has caused -0.487 ± 0.001 μM year^{-1} of deoxygenation and contributed to -0.11 ± 0.04 μM year^{-1} of deoxygenation. The remaining -0.19 ± 0.03 μM year^{-1} of NEPIW-driven deoxygenation has been caused by accumulated internal remineralization within this water mass.

While increasing surface ocean temperatures from climate change could cause elevated remineralization rates, this factor is likely not responsible for the increased accumulation of internal remineralization within the NEPIW, as transit times for NEPIW to reach the ETNP are too long (approximately 55 years; Karstensen et al., 2008) for recent warming trends to have manifested during this observational period. Instead, the internal remineralization observed in the CCS likely occurs nearby, off Mexico. The accumulation rates of internal remineralization in the uPSUW and dPSUW are similar, suggesting processes in the Northeastern Pacific drive the trends for these two water masses (Durski et al., 2017). We suggest that increased subsurface stratification (Rykaczewski & Dunne, 2010) within these waters may be responsible for this deoxygenation trend.

From 1984–2018, the time series of NEPIW contribution to the southern CCS closely fits a linear trend (Figure 2b), even though oscillations such as ENSO impacts the NEPIW contribution by approximately 10% (Bograd et al., 2019). It is likely that our data treatment averaged out the impact of this oscillation. Therefore, repeating this type of deoxygenation deconvolution for specific lines and stations of interest in the CCS will likely provide more nuanced information. In the northern CCS, subsurface deoxygenation appears to be more severe (Chan et al., 2008; Connolly et al., 2010). Internal remineralization accumulated within the NEPIW causes 19% of the deoxygenation in the southern CCS, and this deoxygenation may be greater in the northern CCS due to increased remineralization that occurs during the transit of this water mass in the CUC. Nevertheless, the deoxygenation in the northern CCS may be driven more by upwelling of low O_2 waters than remineralization inside a specific water mass. We recommend replicating the water mass analysis performed in Bograd et al. (2019) and the deoxygenation deconvolution described in this paper for other time series in the CCS, such as the Newport Hydrographic line off Oregon, as well as the Humboldt, Benguela, and Canary Eastern Boundary Upwelling Systems. The Humboldt system shares the same uPEW and similar dPEW as the CCS (Evans et al., 2020), facilitating this investigation.

This study aimed to quantify the relative contributions of advection, remineralization, and the six source water masses in driving deoxygenation in the southern, subsurface CCS. Laffoley and Baxter (2019) estimated that the concentration threshold for coastal low oxygen zones is 60 μM. If equatorial wind stress continues to increase (Deutsch et al., 2014) and this causes deoxygenation to continue linearly at the rates calculated in this study, the 150–325 m depth range of the NEPIW will reach this threshold in 2034. Waters deeper than this threshold have minimal NEPIW contribution and therefore will deoxygenate slower than this rate. We have revealed that in the southern, subsurface CCS, 81% of the observed deoxygenation from 1993–2018 occurred through the southern boundary and at the depths of the NEPIW. This improved understanding of the mechanisms affecting the aerobic habitat of the CCS will inform biogeochemical modeling, allowing improved projections of ecological impacts and mitigation of future deoxygenation.

Conflict of Interest

The authors declare no conflicts of interest.

Data Availability Statement

This study did not use any new data, rather, it reprocessed the CalCOFI data set. The original CalCOFI data are available online (http://www.calcofi.org). The MATLAB OMP toolbox used to generate water mass

contributions in Bograd et al. (2019) is available online (https://www.mathworks.com/matlabcentral/fileexchange/1334-omp-analysis). The MATLAB code for linear regression can be found as attached electronic content for Doney et al. (2012) online (https://www.cambridge.org/us/academic/subjects/earth-and-environmental-science/oceanography-and-marine-science/modeling-methods-marine-science?format=HB).

Acknowledgments
We acknowledge the quality and longevity of the CalCOFI program and the many scientists and seagoing staff who have contributed to the collection, processing, and analysis of this excellent data set. We also acknowledge the California Current Ecosystem Long-Term Ecosystem Research (CCE-LTER) project, supported by a grant from NSF (OCE-0417616). We would like to acknowledge Donald M. Glover, William J. Jenkins, and Scott C. Doney for writing *Modeling Methods for Marine Science* and Naomi Levine for teaching her course on MATLAB, which included this textbook. We appreciate clarifying feedback by Ryan Rykaczewski during internal NOAA review and Jack Barth for review of this submission.

References

Anderson, L. A., & Sarmiento, J. L. (1994). Redfield ratios of remineralization determined by nutrient data analysis. *Global Biogeochemical Cycles*, *8*(1), 65–80. https://doi.org/10.1029/93GB03318

Barbier, E. B. (2017). Marine ecosystem services. *Current Biology*, *27*(11), R507–R510. https://doi.org/10.1016/j.cub.2017.03.020

Bograd, S. J., Buil, M. P., Lorenzo, E. D., Castro, C. G., Schroeder, I. D., Goericke, R., et al. (2015). Changes in source waters to the Southern California Bight. *Deep Sea Research Part II: Topical Studies in Oceanography*, *112*, 42–52. https://doi.org/10.1016/j.dsr2.2014.04.009

Bograd, S. J., Castro, C. G., Lorenzo, E. D., Palacios, D. M., Bailey, H., Gilly, W., & Chavez, F. P. (2008). Oxygen declines and the shoaling of the hypoxic boundary in the California current. *Geophysical Research Letters*, *35*, L12607. https://doi.org/10.1029/2008GL034185

Bograd, S. J., Schroeder, I. D., & Jacox, M. G. (2019). A water mass history of the Southern California current system. *Geophysical Research Letters*, *46*, 6690–6698. https://doi.org/10.1029/2019GL082685

Bostock, H. C., Opdyke, B. N., & Williams, M. J. M. (2010). Characterising the intermediate depth waters of the Pacific Ocean using δ13C and other geochemical tracers. *Deep Sea Research Part I: Oceanographic Research Papers*, *57*(7), 847–859. https://doi.org/10.1016/j.dsr.2010.04.005

Breitburg, D., Levin, L. A., Oschlies, A., Grégoire, M., Chavez, F. P., Conley, D. J., et al. (2018). Declining oxygen in the global ocean and coastal waters. *Science*, *359*(6371), eaam7240. https://doi.org/10.1126/science.aam7240

Brewer, P. G., & Peltzer, E. T. (2016). Ocean chemistry, ocean warming, and emerging hypoxia: Commentary. *Journal of Geophysical Research: Oceans*, *121*, 3659–3667. https://doi.org/10.1002/2016JC011651

Brzezinski, M. A. (1985). The Si:C:N ratio of marine diatoms: Interspecific variability and the effect of some environmental variables. *Journal of Phycology*, *21*(3), 347–357. https://doi.org/10.1111/j.0022-3646.1985.00347.x

Chan, F., Barth, J. A., Lubchenco, J., Kirincich, A., Weeks, H., Peterson, W. T., & Menge, B. A. (2008). Emergence of anoxia in the California current large marine ecosystem. *Science*, *319*(5865), 920–920. https://doi.org/10.1126/science.1149016

Connolly, T. P., Hickey, B. M., Geier, S. L., & Cochlan, W. P. (2010). Processes influencing seasonal hypoxia in the northern California current system. *Journal of Geophysical Research*, *115*, C03021. https://doi.org/10.1029/2009JC005283

Deutsch, C., Berelson, W., Thunell, R., Weber, T., Tems, C., McManus, J., et al. (2014). Centennial changes in North Pacific anoxia linked to tropical trade winds. *Science*, *345*(6197), 665–668. https://doi.org/10.1126/science.1252332

Deutsch, C., Ferrel, A., Seibel, B., Portner, H.-O., & Huey, R. B. (2015). Climate change tightens a metabolic constraint on marine habitats. *Science*, *348*(6239), 1132–1135. https://doi.org/10.1126/science.aaa1605

Doney, S. C., Ruckelshaus, M., Emmett Duffy, J., Barry, J. P., Chan, F., English, C. A., et al. (2012). Climate change impacts on marine ecosystems. *Annual Review of Marine Science*, *4*(1), 11–37. https://doi.org/10.1146/annurev-marine-041911-111611

Durski, S. M., Barth, J. A., McWilliams, J. C., Frenzel, H., & Deutsch, C. (2017). The influence of variable slope-water characteristics on dissolved oxygen levels in the northern California Current System. *Journal of Geophysical Research: Oceans*, *122*, 7674–7697. https://doi.org/10.1002/2017JC013089

Evans, N., Boles, E., Kwiecinski, J. V., Mullen, S., Wolf, M., Devol, A. H., et al. (2020). The role of water masses in shaping the distribution of redox active compounds in the Eastern Tropical North Pacific oxygen deficient zone and influencing low oxygen concentrations in the eastern Pacific Ocean. *Limnology and Oceanography*. https://doi.org/10.1002/lno.11412

Fiedler, P. C., & Talley, L. D. (2006). Hydrography of the eastern tropical Pacific: A review. *Progress in Oceanography*, *69*(2–4), 143–180. https://doi.org/10.1016/j.pocean.2006.03.008

Garcia, H. E., Locarnini, R. A., Boyer, T. P., Antonov, J. I., Mishonov, A. V., Baranova, O. K., et al. (2013). World Ocean Atlas 2013. In S. Levitus (Ed.), A. Mishonov (Technical Ed.), *Vol. 3: Dissolved oxygen, apparent oxygen utilization, and oxygen saturation*, *NOAA Atlas NESDIS* (Vol. 75, p. 27). https://doi.org/10.7289/V5XG9P2W

García-Ibáñez, M. I., Pardo, P. C., Carracedo, L. I., Mercier, H., Lherminier, P., Ríos, A. F., & Pérez, F. F. (2015). Structure, transports and transformations of the water masses in the Atlantic Subpolar Gyre. *Progress in Oceanography*, *135*, 18–36. https://doi.org/10.1016/j.pocean.2015.03.009

Glover, D. M., Jenkins, W. J., & Doney, S. C. (2011). *Modeling Methods for Marine Science*. Cambridge: Cambridge University Press. https://doi.org/10.1017/CBO9780511975721

Gruber, N. (2011). Warming up, turning sour, losing breath: Ocean biogeochemistry under global change. *Philosophical Transactions of the Royal Society A: Mathematical, Physical and Engineering Sciences*, *369*(1943), 1980–1996. https://doi.org/10.1098/rsta.2011.0003

Howard, E. M., Penn, J. L., Frenzel, H., Seibel, B. A., Bianchi, D., Renault, L., et al. (2020). Climate-driven aerobic habitat loss in the California Current System. *Science Advances*, *6*(20), eaay3188. https://doi.org/10.1126/sciadv.aay3188

Karstensen, J., Stramma, L., & Visbeck, M. (2008). Oxygen minimum zones in the eastern tropical Atlantic and Pacific oceans. *Progress in Oceanography*, *77*(4), 331–350. https://doi.org/10.1016/j.pocean.2007.05.009

Karstensen, J., & Tomczak, M. (1997). Ventilation processes and water mass ages in the thermocline of the southeast Indian Ocean. *Geophysical Research Letters*, *24*(22), 2777–2780. https://doi.org/10.1029/97GL02708

Keeling, R. F., Körtzinger, A., & Gruber, N. (2010). Ocean deoxygenation in a warming world. *Annual Review of Marine Science*, *2*(1), 199–229. https://doi.org/10.1146/annurev.marine.010908.163855

Koslow, J., Goericke, R., Lara-Lopez, A., & Watson, W. (2011). Impact of declining intermediate-water oxygen on deepwater fishes in the California Current. *Marine Ecology Progress Series*, *436*, 207–218. https://doi.org/10.3354/meps09270

Koslow, J. A., Goericke, R., & Watson, W. (2013). Fish assemblages in the Southern California Current: Relationships with climate, 1951–2008. *Fisheries Oceanography*, *22*(3), 207–219. https://doi.org/10.1111/fog.12018

Laffoley, D., & Baxter, J. M. (Eds.) (2019). *Ocean deoxygenation: Everyone's problem. Causes, impacts, consequences and solutions*. Gland, Switzerland: IUCN, International Union for Conservation of Nature. https://doi.org/10.2305/IUCN.CH.2019.13.en

Levin, L. A. (2018). Manifestation, drivers, and emergence of open ocean deoxygenation. *Annual Review of Marine Science*, *10*, 229–260. https://doi.org/10.1146/annurev-marine-121916-063359

McClatchie, S., Goericke, R., Cosgrove, R., Auad, G., & Vetter, R. (2010). Oxygen in the Southern California Bight: Multidecadal trends and implications for demersal fisheries: Oxygen trends Southern California Bight. *Geophysical Research Letters*, *37*, L19602. https://doi.org/10.1029/2010GL044497

Meinvielle, M., & Johnson, G. C. (2013). Decadal water-property trends in the California Undercurrent, with implications for ocean acidification. *Journal of Geophysical Research: Oceans*, *118*, 6687–6703. https://doi.org/10.1002/2013JC009299

Nam, S., Takeshita, Y., Frieder, C. A., Martz, T., & Ballard, J. (2015). Seasonal advection of Pacific Equatorial Water alters oxygen and pH in the Southern California Bight. *Journal of Geophysical Research: Oceans*, *120*, 5387–5399. https://doi.org/10.1002/2015JC010859

National Geophysical Data Center (2006). 2-minute Gridded Global Relief Data (ETOPO2) v2. National Geophysical Data Center, NOAA. https://doi.org/10.7289/V5J1012Q

Poole, R., & Tomczak, M. (1999). Optimum multiparameter analysis of the water mass structure in the Atlantic Ocean thermocline. *Deep Sea Research Part I: Oceanographic Research Papers*, *46*(11), 1895–1921. https://doi.org/10.1016/S0967-0637(99)00025-4

Qu, T., Gao, S., Fukumori, I., Fine, R. A., & Lindstrom, E. J. (2009). Origin and pathway of equatorial 13°C water in the Pacific identified by a simulated passive tracer and its adjoint. *Journal of Physical Oceanography*, *39*(8), 1836–1853. https://doi.org/10.1175/2009JPO4045.1

Rykaczewski, R. R., & Dunne, J. P. (2010). Enhanced nutrient supply to the California Current Ecosystem with global warming and increased stratification in an earth system model. *Geophysical Research Letters*, *37*, L21606. https://doi.org/10.1029/2010GL045019

Tomczak, M., & Large, D. G. B. (1989). Optimum multiparameter analysis of mixing in the thermocline of the eastern Indian Ocean. *Journal of Geophysical Research*, *94*(C11), 16,141–16,149. https://doi.org/10.1029/JC094iC11p16141

Tsuchiya, M. (1981). The origin of equatorial 13 C water. *Journal of Physical Oceanography*, *11*, 794–812. https://doi.org/10.1175/1520-0485(1981)011%3C0794:TOOTPE%3E2.0.CO;2